

# Green Synthesis of Fe<sub>3</sub>O<sub>4</sub> Magnetic Nanoparticle by *Moringa oleifera* Leaf Extract for Photocatalytic of Congo Red dye

Fahma Riyanti<sup>1</sup>, Fitria Nursari<sup>2</sup>, Bijak Riyandi Ahadito<sup>3</sup>, Laila Hanum<sup>4</sup>, Eliza<sup>5</sup> and Poedji Loekitowati Hariani<sup>6</sup>

{fatechafj@unsri.ac.id<sup>1</sup>, fitrianursari12@gmail.com<sup>2</sup>, bijak@mipa.unsri.ac.id<sup>3</sup>, lailahanum@unsri.ac.id<sup>4</sup>, elizapalembang2023@gmail.com<sup>5</sup>, puji\_lukitowati@mipa.unsri.ac.id<sup>6</sup>}

Research Group on Magnetic Materials, Department of Chemistry, Faculty of Mathematics and Natural Sciences, Universitas Sriwijaya, Ogan Ilir 30662, Indonesia<sup>1,2</sup>  
Department of Chemistry, Faculty of Mathematics and Natural Sciences, Universitas Sriwijaya, Ogan Ilir 30662, Indonesia<sup>1,2,3,5,6</sup>  
Department of Biology, Faculty of Mathematics and Natural Sciences, Universitas Sriwijaya, Ogan Ilir 30662, Indonesia<sup>4</sup>

Corresponding author: [fatechafj@unsri.ac.id](mailto:fatechafj@unsri.ac.id)

**Abstract.** Natural water resources can be contaminated if industrial waste is inadequately treated. The uncontrolled release of dangerous organic compounds poses a serious environmental risk. Before wastewater may be discharged into the environment, it must be processed properly. The green synthesis method, *Moringa oleifera* leaf extract, was used in this study to produce Fe<sub>3</sub>O<sub>4</sub> (magnetite). The green synthesis method is an environmentally friendly, cost-effective, low-toxicity, and simple method. Following that, Fe<sub>3</sub>O<sub>4</sub> was used to photodegrade Congo red dye. XRD, SEM-EDX, VSM, UV-Vis DRS, and FTIR were used to characterize Fe<sub>3</sub>O<sub>4</sub> products. pH of the solution, dye concentration, and irradiation time are photodegradation variables. The resulting Fe<sub>3</sub>O<sub>4</sub> is magnetic, with a saturation magnetization value of 80.25 emu/g and a band gap energy of 1.42 eV. At a solution pH of 3, Congo red concentration of 50 mg/L, and an irradiation time of 30 minutes, the photodegradation effectiveness was 98.55%. After five consecutive reuse cycles, Fe<sub>3</sub>O<sub>4</sub> shows outstanding photostability. According to the findings of this study, Fe<sub>3</sub>O<sub>4</sub> is particularly promising for processing dye-containing waste.

**Keywords:** green synthesis, Fe<sub>3</sub>O<sub>4</sub>, photodegradation, Congo red.

## 1 Introduction

If increasing industrialization is not balanced with refuse management, it will have a negative impact on the environment and on living things [1]. The majority of pollutants are stable organic compounds that are extremely toxic. This dye is utilized in numerous industries, including textiles, detergents, paper, cosmetics, and printing. About of 20-40% of the industrially used dyes are azo dyes [2]. The characteristic group of azo dyes is -N=N- bond. Azo dyes have negative effects such as biotoxicity, carcinogenicity, causing allergies, skin and ocular irritation

and diminishing aesthetic appeal [3]. Congo red dye is one of these dyes. This dye has the molecular formula  $C_{32}H_{22}N_6Na_2O_6S_2$ , is anionic, contains an aromatic group and two azo groups, and is water-soluble [3,4]. The complex aromatic structure of Congo red dye makes its degradation in the environment problematic [5]. It is crucial to remove the Congo red pigment before releasing it into the environment.

Several techniques, including chemical oxidation [6], chlorination [7], ozonation [8], adsorption [9] and photocatalysis [10], have been utilized to eliminate dye concentrations. The photocatalytic degradation of semiconductors has garnered considerable interest. This process involves the formation of hydroxyl radicals when UV or visible light is present [11]. The oxidation and mineralization of organic pollutants into innocuous compounds such as  $CO_2$  and  $H_2O$  [10].

The general formula for ferrite compounds is  $MF_2O_4$  (M is a divalent metal cation). Ferrite compounds have excellent chemical properties and stability, as well as high permeability, biocompatibility, and magnetic moment [12,13]. Ferrite compounds are semiconducting materials with a band gap of approximately 2 eV and the ability to absorb visible light. The magnetic properties of ferrite compounds are advantageous to the photocatalytic process because a permanent magnet can be used to rapidly separate the catalyst [10].  $Fe_3O_4$  (magnetic) is a ferrite compound with distinctive properties, including environmental compatibility, minimal toxicity, large surface area, and superparamagnetic [14,15]. It is important to modify  $Fe_3O_4$  to prevent aggregation and oxidation by atmospheric oxygen [16].

Green synthesis is a low-cost, non-toxic, ecologically friendly, and dependable material synthesis technique that uses fungi and bacteria along with plant extracts. Polyphenols, terpenoids, flavonoids, polyols, aldehydes, ketones, amides, carboxylic acids, and ascorbic acid found in plant extracts function as capping agents and bio reductors, producing particles with a size range of 1-100 nm [17]. The ferrite nanoparticles through chemical means have detrimental impacts on the environment and on biological systems.  $Fe_3O_4$  has been synthesized utilizing a variety of plant extracts, such as rind extract from *Punica granatum* [18], *Citrus aurantium* [19], and *Sapindus mukkorossi* fruits [20]. The 'drumstick' tree, *Moringa oleifera* Lam, is a member of the *Moringaceae* family and is recognized for its significant nutritional value [21]. Protein, carbohydrates, phenols, vitamins, kaempferol, potassium, calcium, amino acids, and essential oils are all present in *Moringa oleifera* plant extract [21,22].

In this study, we investigated the green synthesis of  $Fe_3O_4$  nanoparticles using the leaf extract of *Moringa oleifera*, which is used for photocatalytic Congo red dye. The photocatalytic variables include solution pH, dye concentration and irradiation time. Produced  $Fe_3O_4$  was characterized by means of XRD, SEM-EDS, UV-DRS, VSM, and FTIR.

## 2 Material and Methods

### 2.1. Materials

The materials used include  $FeCl_3$ ,  $FeSO_4 \cdot 7H_2O$ ,  $C_2H_5OH$ ,  $CHCl_3$ ,  $NaNO_3$ ,  $NaOH$ , dandedorf reagent from Merck, Congo red from Sigma Aldrich, *Moringa oleifera* leaves from Indralaya, Ogan Ilir, Indonesia.

## **2.2. Preparation of *Moringa Oleifera* leaf extract**

For three days, about 100 grams of *Moringa Oleifera* leaf powder was soaked in 500 milliliters of ethanol. This made a light brown solution. The soak was filtered through Whatman filter paper, and the filtrate was evaporated in a rotating evaporator set to 60°C and 30 rpm to get a thick extract.

## **2.3. Synthesis Fe<sub>3</sub>O<sub>4</sub> nanoparticle**

In this experiment, a solution was prepared by dissolving 3.25 g of FeCl<sub>3</sub> and 2.78 g of FeSO<sub>4</sub>·7H<sub>2</sub>O separately in 50 mL of distilled water. The mixture received an addition of 3 mL of *Moringa oleifera* leaf extract. The solution was subjected to heating at a temperature of 60°C and agitation was achieved by employing a magnetic stirrer operating at a rotational speed of 450 rpm. Concurrently, 2 M of NaOH solution was incrementally introduced into the mixture until the pH level approached around 10. The resulting solid was subjected to filtration and subsequently washed with distilled water until a neutral pH of 7 was achieved. Subsequently, the precipitate underwent a drying process in an oven set at a temperature of 80°C for a duration of 2 h.

## **2.4. Characterization**

X-Ray Diffraction (XRD) PANalytical type X'Pert PRO) used to determine the crystal size and nanoparticle phase, where Cu-K $\alpha$  ( $\lambda = 1,5406 \text{ \AA}$ ) dan  $2\theta = 10-80^\circ$ . The morphology and composition of the elements were evaluated using Scanning Electron Microscope-Energy Dispersive X-ray (SEM-EDX) JOEL JSM-6510 LA, Vibrating Sample Magnetometer (VSM) Oxford Type 1.2 T to determine magnetic properties, bandgap of Fe<sub>3</sub>O<sub>4</sub> nanoparticles was determined using Ultraviolet-Visible Diffuse Reflectance Spectrum (UV-Vis DRS) Pharmaspec UV-1700, and functional groups analyzed using Fourier Transform Infra-Red (FTIR) Prestige 21 Shimadzu at wave numbers 4000-400 cm<sup>-1</sup>. Congo red dye concentration was determined using an Orion Aquamate 8000 UV-Vis spectrophotometer. TOC analysis was carried out using a Teledyne Tekmar TOC torch type TOC analyzer.

## **2.5. Determination of pH Point Zero Charge (pH pzc)**

In each Erlenmeyer flask, 50 mL of 0.01 M NaNO<sub>3</sub> solution was placed. The pH was changed by adding 0.1 M HNO<sub>3</sub> or 0.1 M NaOH solution. The pH was lowered to a range of 2 to 11. Each Erlenmeyer flask was then filled with 0.05 g of Fe<sub>3</sub>O<sub>4</sub> nanoparticles. A shaker was used to agitate the mixture for 2 hours. The mixture was then allowed for two days to calculate the difference between the initial and final pH values.

## **2.6. Photocatalytic activity**

Using a 300 W UV light source, photocatalytic activity is conducted within a photocatalyst reactor. The distance between the lamp and the solution is 10 cm. The volume of the used dye solution was 25 mL, and Fe<sub>3</sub>O<sub>4</sub> nanoparticles was 0.05 g. Photocatalysis variables consist of Congo red dye pH (2-7) and concentration (25-150 mg/L), as well as irradiation time (10-60 minutes). In this study the same process was carried out but without irradiation.

### 3 Result and Discussion

#### 3.1. Characterization of Fe<sub>3</sub>O<sub>4</sub> nanoparticle

The X-ray diffraction (XRD) spectra of Fe<sub>3</sub>O<sub>4</sub> nanoparticles are depicted in Figure 1(a). The diffraction patterns obtained exhibit angles of  $2\theta = 30.29^\circ, 35.50^\circ, 43.15^\circ, 53.51^\circ, 57.10^\circ,$  and  $62.75^\circ$ , corresponding to the plane indices (220), (311), (400), (422), (511), and (440). The peak under consideration has an inverse spinel structure, as shown by the JCPDS cards No. 74-0748. The average diameters of Fe<sub>3</sub>O<sub>4</sub> nanoparticles, as determined using the Debye-Scherrer formula, were found to be 22.71 nm. Particles ranging from 1 to 100 nanometers in size are categorized as nanoscale entities. Additional studies have demonstrated a correlation between the quantity of *Garcinia mangostana* fruit peel employed in the synthesis of Fe<sub>3</sub>O<sub>4</sub> and its impact on crystallinity and particle size. It has been observed that an increase in the mass of *Garcinia mangostana* fruit peel (1, 2, 5, and 10 % wt) leads to a corresponding increase in crystallinity and a decrease in particle size [23].

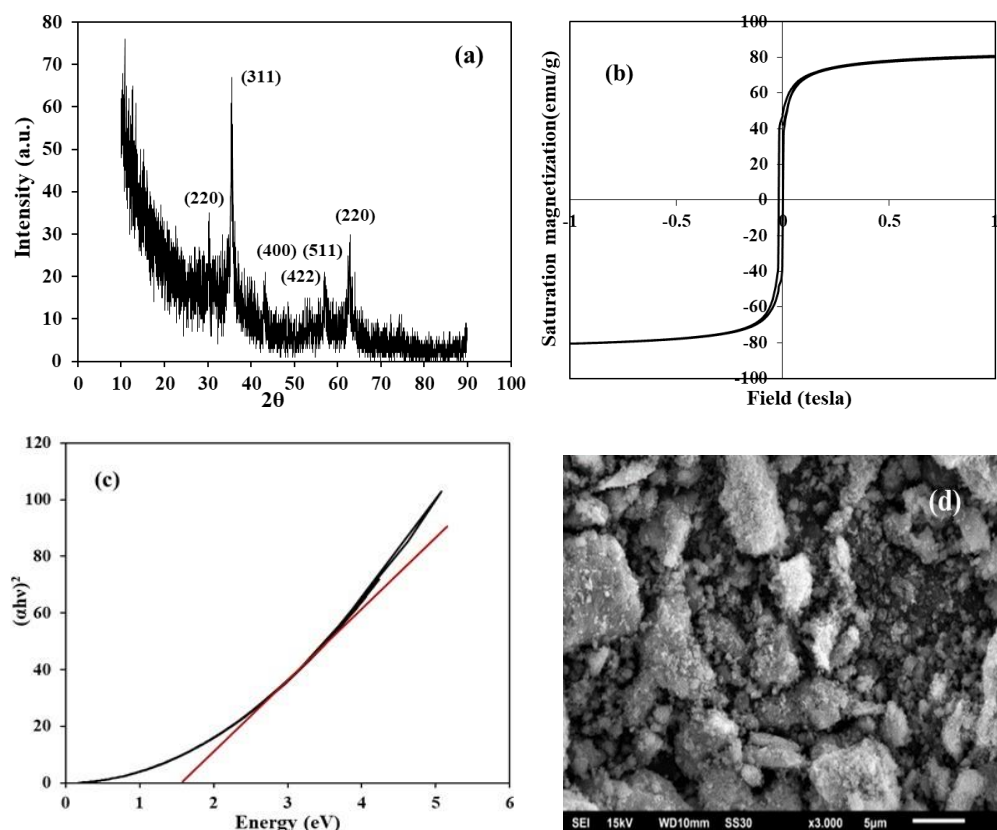


**Fig. 1.** a) XRD pattern, b) morphology c) magnetic properties, and d) Uv-DRS of Fe<sub>3</sub>O<sub>4</sub> nanoparticle

Based on the hysteresis curve in Figure 2(b), the Fe<sub>3</sub>O<sub>4</sub> nanoparticles have a saturation

magnetization (Ms) of 80.25 emu/g. The saturation magnetization value obtained in this study is greater than that of Fe<sub>3</sub>O<sub>4</sub> synthesized by the hydrothermal method, which is 73.87 emu/g [24]. The capping process with non-magnetic compounds results in a decrease in saturation magnetization, with the saturation magnetization of bulk Fe<sub>3</sub>O<sub>4</sub> being 92 emu/g [25]. The energy bandgap value of the Fe<sub>3</sub>O<sub>4</sub> nanoparticles is 1.42 eV, as shown in Figure 2(c). The energy bandgap of Fe<sub>3</sub>O<sub>4</sub> nanoparticles is determined from the plot of  $[F(R) \times hv]^2$  vs energy. The ferrite compounds have a band gap value of around 2.0 eV, which is effective for absorbing visible light [26].

Figure 2(d) displays the morphology of Fe<sub>3</sub>O<sub>4</sub> nanoparticles as analyzed using SEM. The Fe<sub>3</sub>O<sub>4</sub> nanoparticles appear to be small, spherical, resembling balls, but there are also elongated, shard-like shapes. These results are consistent with what was reported by Ravindra et al [27], as the effect of capping or surfactant added during synthesis can result in diverse shapes. Table 1 shows the elemental composition of the Fe<sub>3</sub>O<sub>4</sub> nanoparticle as determined by EDX analysis. The success of the synthesis is indicated by the presence of Fe and O elements originating from Fe<sub>3</sub>O<sub>4</sub> nanoparticle, as well as C and S elements from the *Moringa oleifera* leaf extract.

**Table 1.** Composition of Fe<sub>3</sub>O<sub>4</sub> nanoparticles from EDX analysis

Elements	Atomic (%)
Fe	35.96
O	37.54
C	25.83
S	0.67

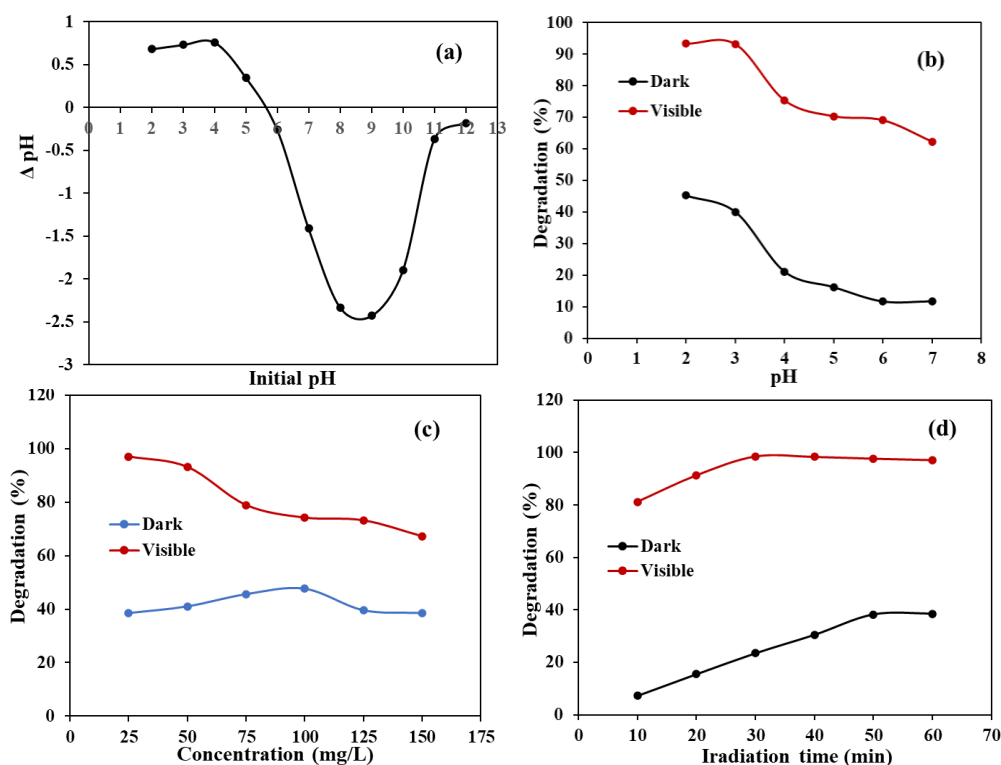
### 3.2. Optimization of photocatalytic

To investigate the photocatalytic activity of Fe<sub>3</sub>O<sub>4</sub> nanoparticles, experiments were carried out using the batch method with several variables, namely the pH of the solution, dye concentration and irradiation time. pH plays an important role in the photocatalytic degradation process. pH pzc is the pH value at which the surface of a material or solid particle has a neutral charge, or the ionization and deionization rates on the surface are balanced. If the pH of the solution is above pH pzc then the surface of the material has a negative charge (-) and vice versa. The pH of pzc Fe<sub>3</sub>O<sub>4</sub> nanoparticles is 5.6, as depicted in Figure 2(a).

The effect of pH on the solution was conducted using a Congo red dye concentration of 50 mg/L with a volume of 25 mL and an irradiation time of 60 minutes within the pH range of 2-8. Figure 2(b) shows that at solution pH values below the pH pzc, the degradation percentage is higher compared to solution pH values above pH pzc. Fe<sub>3</sub>O<sub>4</sub> nanoparticles are positively charged at solution pH values below pH pzc, while Congo red dye is an anionic dye, making electrostatic attraction more effective. Adsorption is the initial process before degradation occurs. Solution pH values of 2 and 3 are the optimal pH levels, which align with the findings reported by Fahma et al. [28] in the photocatalytic degradation of Congo red dye using bentonite-Fe<sub>3</sub>O<sub>4</sub> composite.

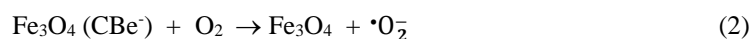
The determination of the concentration effect was carried out at dye concentrations of 25, 50, 75, 100, 125, and 150 mg/L, as shown in Figure 2(c). A 25 mL volume of dye was adjusted to a pH of 3 with a 60 minute irradiation time. The 25 mg/L concentration exhibited the highest degradation percentage, which is 94.35%. As the concentration increased, the degradation percentage decreased. The number of active sites on the catalyst's surface, namely hydroxyl radicals ( $\bullet$ OH), is limited, while the concentration of the dye being degraded increases, resulting

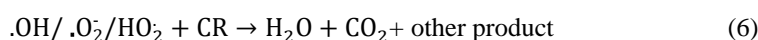
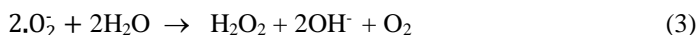
in a decrease in degradation efficiency [10,28].



**Fig. 2.** a) pH pzc of  $\text{Fe}_3\text{O}_4$  nanoparticle, and effect of b) solution pH, c) concentration of dye and d) irradiation time in photocatalytic of Congo red dye

The effect of irradiation time was determined by modifying the duration of exposure to 10, 20, 30, 40, 50, and 60 minutes. The concentration of Congo red dye was 25 mg/L and the pH was adjusted to 3. Figure 2(d) demonstrates that the longer the irradiation, the greater the percentage of degradation, but after 40 minutes there was no change in the percentage of degradation. The degradation percentage obtained was 98.55%. This phenomenon demonstrates that deterioration occurs rapidly. Following is the proposed mechanism for the degradation of Congo red dye as follow: [29,30]





The percentage removal of Congo red dye concentration is significantly higher when irradiation is involved, indicating that visible irradiation is a crucial factor in the degradation process. The degradation mechanism involves the formation of radicals  $\cdot\text{OH}$ ,  $\cdot\text{O}_2^-$ , and  $\text{HO}_2$  which play pivotal roles in this process. When the photocatalyst absorbs light, it acquires energy, which is utilized to excite electrons from the valence band (VB) to the conduction band (CB). This process generates a hole in the VB ( $\text{h}^+$ ) and an electron in the CB ( $\text{e}^-$ ). Subsequently, these holes break down water molecules, forming hydroxyl radicals that react with organic molecules to break down organic compounds [31].

The reusability of  $\text{Fe}_3\text{O}_4$  nanoparticles as a catalyst is illustrated in Figure 3. The photocatalytic degradation process was conducted under optimal conditions for 5 cycles.  $\text{Fe}_3\text{O}_4$  nanoparticles exhibited commendable stability and performance, with only a slight decrease in the degradation percentage of 4.35% after 5 cycles of use. Notably, research conducted by Zhang et al. [32] demonstrated the reusability of  $\text{Fe}_3\text{O}_4$  nanoparticles in the degradation of naphthalene for up to 4 cycles, with a decrease in the degradation percentage of less than 5%. This decrease in degradation percentage was primarily attributed to the loss of  $\text{Fe}_3\text{O}_4$  nanoparticles during the regeneration process. These findings underscore the excellent potential of  $\text{Fe}_3\text{O}_4$  as a photocatalyst.

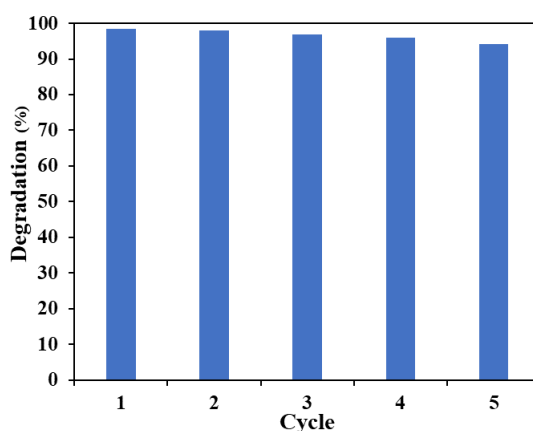


**Fig. 3.** Reusability of  $\text{Fe}_3\text{O}_4$  nanoparticle for photocatalytic degradation of Congo red dye

Total Organic Carbon measurements are carried out to determine the amount of carbon contained in the sample. The effectiveness of reducing the carbon concentration in Congo red dye can be determined by comparing the amount of carbon in the dye before and after photodegradation using  $\text{Fe}_3\text{O}_4$  nanoparticle. This study obtained a TOC value of 74.75%, indicating that

mineralization of the dye has occurred.

### 3.3. FTIR spectra of Fe<sub>3</sub>O<sub>4</sub> nanoparticle

Figure 4 displays the FTIR spectrum of Fe<sub>3</sub>O<sub>4</sub> nanoparticles in the wave number range of 4000-400 cm<sup>-1</sup>. Notably, there is no significant difference in the FTIR spectra of Fe<sub>3</sub>O<sub>4</sub> nanoparticles observed before and after their use in the photocatalytic degradation process. This observation indicates that Fe<sub>3</sub>O<sub>4</sub> nanoparticles exhibit high stability. The wave number within the range of 3600-3100 cm<sup>-1</sup> signify the stretching vibration of the hydroxyl (O-H) group, which originates from both water and compounds present in the *Moringa Oleifera* leaf extract. Additionally, there is absorption around 2900 cm<sup>-1</sup>, indicating bonds within the C-H group. These bonds are associated with various compounds like phenolics, terpenoids, and phenolic acids. A sharp band around 1600 cm<sup>-1</sup> corresponds to the stretching and bending of the N-H bond [33]. Meanwhile, the absorption peak at 1110 cm<sup>-1</sup> is linked to alkoxy C-O stretching vibrations, which are characteristic of oxygen-containing functional groups such as carbonyl, carboxylic, and epoxy groups [34]. Aliphatic and aromatic carbon are also observable as sharp signals in the ranges of 1400-1500 cm<sup>-1</sup> and approximately 1250 cm<sup>-1</sup>.

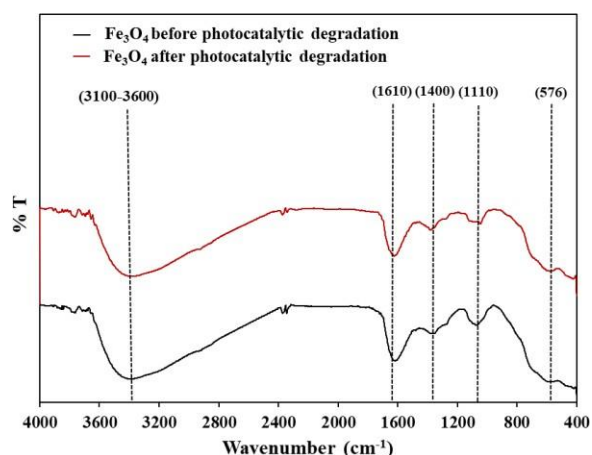


Fig. 4. FTIR spectra of Fe<sub>3</sub>O<sub>4</sub> nanoparticle

## 4 Conclusion

In this research, Fe<sub>3</sub>O<sub>4</sub> nanoparticles were successfully synthesized through a green synthesis method involving the use of *Moringa oleifera* leaf extract. The resulting nanoparticles exhibited magnetic properties, which conferred a significant advantage in the separation process. After the photocatalytic degradation process, these nanoparticles could be rapidly separated from the solution using a permanent magnet. The application of these nanoparticles in the photocatalytic degradation of Congo red dye demonstrated a high efficiency of 95.88%. Furthermore, the Fe<sub>3</sub>O<sub>4</sub> nanoparticles displayed remarkable stability as evidenced by the reusability tests, indicating that even after up to 5 cycles of the photocatalytic degradation process, the degradation percentage decreased by less than 5%. This stability was also supported by the FTIR spectra analysis before and after degradation, which showed no significant peak changes. In conclusion, the Fe<sub>3</sub>O<sub>4</sub>



nanoparticles have substantial potential for application in treating liquid waste, particularly those containing dyes, due to their efficient photocatalytic properties, stability, and the ease of separation using magnetic properties.

## Acknowledgments

The author would like to thank the research funding through DIPA of Publics Service Agency of Universitas Sriwijaya 2023, SP DIPA-023.17.2.677515/2023, on November 2022. In accordance with Dean's decree Number. 0009/UN9.FMIPA/TU.SK/2023, on June 13, 2023.

## References

- [1] Yadav, A., Dhariwal, A., Kumari., M., Kumar, V., Thakur, O.P.: Enhanced degradation of Congo-red dye by Cr<sup>3+</sup> doped  $\alpha$ -Fe<sub>2</sub>O<sub>3</sub> nanoparticles under sunlight and industrial wastewater treatment. *Chemosphere*. Vol. 343, pp. 1-10 (2023)
- [2] Sillanpa, M., Mahvi, A.H., Balarak, D., Khatibi, A.D.: Adsorption of Acid orange 7 dyes from aqueous solution using polypyrrole/nanosilica composite: experimental and modelling. *International Journal of Environmental Analytical Chemistry*. Vol. 103. No. 1. pp. 212-229 (2023)
- [3] Al-Hawary, S.I.S., Rahimpoor, R., Rahmani, A., Romero-Parra, R.M., Ramírez-Coronel, A.A., Alhachami, F.R., Mengelizadeh, N., Balarak, D.: Enhanced sonophotocatalytic degradation of acid red 14 using Fe<sub>3</sub>O<sub>4</sub>@SiO<sub>2</sub>/PAEDTC@MIL-101 (Fe) based on metal-organic framework. *Catalysts*. Vol. 13. No. 2. pp. 1-19 (2023)
- [4] Kadari, A.S., Khane, Y., Ech-Chergui, A.N., Popa, A., Guezzoul, M., Silipas, D., Bennabi, F., Zoukel, A., Akyildiz, E., Driss-Khodja, K., Amrani, B.: Growth, properties and photocatalytic degradation of congo red using Gd:ZnO thin films under visible light. *Inorganic Chemistry Communication*. Vol. 142. pp. 1-11 (2022)
- [5] Abdollahi, Y., Abdullah, A.H., Zainal, Z., Yusof, N.A.: Photocatalytic degradation of p-Cresol by zinc oxide under UV irradiation. *International Journal of Molecular Sciences*. Vol. 13. pp. 302-315. (2012)
- [6] Zaheer, Z., Al-Shehri, A.S., Alsudairi, A.M., Kosa, S.A.: Silver-ruthenium bimetallic nanoparticles as sacrificial heterogeneous persulfate activator in situ chemical oxidation of dye. *Journal of Molecular Liquids*. Vol. 377. pp 1-11 (2023)
- [7] Peng, W., Fu, Y., Wang, L., Wang, Y., Dong, Y., Huang, Y., Wang, Z.: Effects of exogenic chloride on oxidative degradation of chlorinated azo dye by UV-activated peroxodisulfate. *Chinese Chemical Letters*. Vol. 3. pp. 2544-2550 (2021)
- [8] Chokshi, N.P., Chauhan, A., Chhayani, R., Sharma, S., Ruparelia, J.P. Preparation and application of AgeCeeO composite metal oxide catalyst in catalytic ozonation for elimination of Reactive Black 5dye from aqueous media. *Water Science and Engineering*. Vol. 48. pp. 1-9 (2023)
- [9] Aftab, R.A., Zaidi, S., Khan, A.A.P., Usman, M.A., Khan, A.Y., Chani, M.T.S., Asiri, A.M.: Removal of Congo red from water by adsorption onto activated carbon derived from waste black cardamom peels and machine learning modeling. *Alexandria Engineering Journal*. Vol. 71. pp. 355-369 (2023)
- [10] Hariani, P.L., Said, M., Rachmat, A., Riyanti, F., Pratiwi, H.C, Rizki, W.T.: Preparation of NiFe<sub>2</sub>O<sub>4</sub> nanoparticles by solution combustion method as photocatalyst of Congo red. *Bulletin of Chemical Reaction Engineering & Catalysis*. Vol. 16. No. 3. pp 481-490 (2021)

- [11] Brame, Q.L., Alvarez, P.J.J.: Nanotechnology-enabled water treatment and reuse: emerging opportunities and challenges for developing countries. *Trends in Food Science & Technology*. Vol. 22. pp. 618-624 (2011)
- [12] Casbeer, V.K. Sharma, X.-Z. Li.: Synthesis and photocatalytic activity of ferrites under visible light: a review. *Separation and Purification Technology*. Vol. 87. pp. 1-14 (2012)
- [13] Donmez, C.E.D., Manna, P.K., Nickel, R., Aktürk, S., Lierop, J.V.: Comparative heating efficiency of cobalt-, manganese-, and nickel-ferrite nanoparticles for a hyperthermia agent in biomedicines. *ACS Applied Materials & Interfaces*. Vol. 11. pp. 6858-6866 (2019)
- [14] Jazirehpour, M., Ebrahimi, S.S.: Effect of aspect ratio on dielectric, magnetic, percolative and microwave absorption properties of magnetite nanoparticles. *Journal of Alloys and Compounds*. Vol. 638. pp. 188-196 (2015)
- [15] Akbarzadeh, A., Samiei, M., Davaran, S.: Magnetic nanoparticles: preparation, physical properties, and applications in biomedicine. *Nanoscale Research Letters*. Vol. 7. pp. 1-13 (2012)
- [16] Wu, W., He, Q., Jiang, C.: Magnetic iron oxide nanoparticles: synthesis and surface functionalization strategies. *Nanoscale Research Letters*. Vol. 3. pp. 397-415 (2008)
- [17] Hussain, I., Singh, N.B., Singh, A., Singh, H., Singh, S.C.: Green synthesis of nanoparticles and its potential application. *Biotechnology Letters*. Vol. 38. pp. 545-560 (2016)
- [18] Venkateswarlu, S., Kumar, B.N., Prathima, B., SubbaRao, Y., Jyothi, N.V.V.: A novel green synthesis of Fe<sub>3</sub>O<sub>4</sub> magnetic nanorods using Punica Granatum rind extract and its application for removal of Pb(II) from aqueous environment. *Arabian Journal of Chemistry*. Vol. 12. No. 40. pp. 588-596 (2019)
- [19] Bassim S., Mageed, A.K., AbdulRazak, A.A., Majdi, H.: Green synthesis of Fe<sub>3</sub>O<sub>4</sub> nanoparticles and its applications in wastewater treatment. *Inorganics*. Vol. 10. No. 20. pp. 1-23 (2022)
- [20] Madhuvilakku, R., Alagar, S., Mariappan, R., Piraman, S.: Green one-pot synthesis of flowers- like Fe<sub>3</sub>O<sub>4</sub>/rGO hybrid nanocomposites for effective electrochemical detection of riboflavin and low-cost supercapacitor applications. *Sensors and Actuators B: Chemical*. Vol. 253. pp. 879-892 (2017)
- [21] Saini, R.K., Sivanesan, I., Keum, Y.: Phytochemicals of *Moringa oleifera*: a review of their nutritional, therapeutic and industrial significance. *3 Biotech*. Vol. 6. No. 203. pp. 1-14 (2016)
- [22] Larasati, D.A., Puspitarum, D.L., Darmawan, M.Y., Istiqomah, N.I., Partini, J., Aliah, H., Suharyadi, E.: Green synthesis of CoFe<sub>2</sub>O<sub>4</sub>/ZnS composite nanoparticles utilizing *Moringa Oleifera* for magnetic hyperthermia applications. *Results in Materials*. Vol. 19. pp. 1-11 (2023)
- [23] Yusefi, M., Shameli, K., Teow, O.S.Y.S., Hedayatnasabb, Z., Jahangirian, H., Webster, T.J., Kuca, K.: Green synthesis of Fe<sub>3</sub>O<sub>4</sub> nanoparticles stabilized by a *Garcinia mangostana* fruit peel extract for hyperthermia and anticancer activities. *International Journal of Nanomedicine*. Vol. 16. pp. 2515-2532 (2021)
- [24] Bojabady, F., Kamali-Heidari, E., Sahebani, S.: Hydrothermal synthesis of highly aligned Fe<sub>3</sub>O<sub>4</sub> nanoslates on nickel foam. *Materials Chemistry and Physics*. Vol. 305. pp. 1-7 (2023)
- [25] Tao K, Dou HJ, Sun K.: Interfacial coprecipitation to prepare magnetite nanoparticles: Concentration and temperature dependence. *Colloids and Surfaces*. Vol. 320. pp.115-122 (2008)
- [26] Casbeer, E., Sharma, V.K., Li, X.Z.: Synthesis and photocatalytic activity of ferrites under visible light: A review. *Separation and Purification Technology*. Vol. 87. 1-14 (2012)
- [27] Ravindra, A.V., Chandrika, M., Sandeep, A.: Superior photocatalytic performance of ancillary-oxidant-free novel starch supported nano MFe<sub>2</sub>O<sub>4</sub> (M = Zn, Ni, and Fe) ferrites for degradation of organic dye pollutants. *Surfaces and Interfaces*. Vol. 41. pp. 1-12 (2023)

- [28] Riyanti, F., Hasanudin, H., Rachmat, A., Purwaningrum, W., Hariani, P.L.: Photocatalytic degradation of Methylene blue and Congo red dyes from aqueous solutions by bentonite-Fe<sub>3</sub>O<sub>4</sub> magnetic. *Communications in Science and Technology*. Vol. 8. No. 1. pp. 1-9 (2023)
- [29] Boulahbel, H., Benamira, M., Bouremmad, F., Ahmia, N., Kiamouche, S., Lahmar, H., Souici, A., Trari, M.: Enhanced photodegradation of Congo red dye under sunlight irradiation by p-n NiFe<sub>2</sub>O<sub>4</sub>/TiO<sub>2</sub> heterostructure. *Inorganic Chemistry Communications*. Vol. 154. pp. 1-12 (2023)
- [30] Talebi, R.: Preparation of nickel ferrite nanoparticles via A new route and study of their photocatalytic properties. *Journal of Materials Science*. Vol. 28. pp. 4058-4063 (2017)
- [31] Sonu, Dutta, V., Sharma, S, Raizada, P., Bandegharai, A.H., Gupta, V.K., Singh, P.: Review on Augmentation in Photocatalytic Activity of CoFe<sub>2</sub>O<sub>4</sub> via Heterojunction Formation for Photocatalysis of Organic Pollutants in Water. *Journal of Saudi Chemical Society*. Vol. 23. pp. 1119-1136 (2019)
- [32] Zhang, J., Fan, S., Lu, B., Cai, Q., Zhao, J., Zang, S.: Photodegradation of naphthalene over Fe<sub>3</sub>O<sub>4</sub> under visible light irradiation. *Royal Society Open Science*. Vol. 6. pp. 1-15 (2018)
- [33] Touqeer, T., Mumtaz, M.W., Mukhtar, H., Irfan, A., Akram, S., Shabbir, A., Rashid, U., Nehdi, I.A., Choong, TSY.: Fe<sub>3</sub>O<sub>4</sub>-PDA-Lipase as Surface Functionalized Nano Biocatalyst for the Production of Biodiesel Using Waste Cooking Oil as Feedstock: Characterization and Process Optimization. *Energies*. Vol. 13. No. 17. pp. 1-19 (2020)
- [34] Chang, C.J., Lee, Z., Chu, K.W., Wei, Y.H.: CoFe<sub>2</sub>O<sub>4</sub>@ZnS core-shell spheres as magnetically recyclable photocatalysts for hydrogen production. *Journal of the Taiwan Institute of Chemical Engineers*. Vol. 66. pp. 386-393 (2016)